World Academy of Science, Engineering and Technology
International Journal of Mechanical and Mechatronics Engineering
Vol:11, No:6, 2017

Unsteady Rayleigh-Bénard Convection of Nanoliquids in Enclosures

P. G. Siddheshwar, B. N. Veena

***Abstract*—**Rayleigh-Bénard convection of a nanoliquid in shallow, square and tall enclosures is studied using the Khanafer-Vafai-Lightstone single-phase model. The thermophysical properties of water, copper, copper-oxide, alumina, silver and titania at $\mathbf{300^0}$ K under stagnant conditions that are collected from literature are used in calculating thermophysical properties of water-based nanoliquids. Phenomenological laws and mixture theory are used for calculating thermophysical properties. Free-free, rigid-rigid and rigid-free boundary conditions are considered in the study. Intractable Lorenz model for each boundary combination is derived and then reduced to the tractable Ginzburg-Landau model. The amplitude thus obtained is used to quantify the heat transport in terms of Nusselt number. Addition of nanoparticles is shown not to alter the influence of the nature of boundaries on the onset of convection as well as on heat transport. Amongst the three enclosures considered, it is found that tall and shallow enclosures transport maximum and minimum energy respectively. Enhancement of heat transport due to nanoparticles in the three enclosures is found to be in the range 3% - 11%. Comparison of results in the case of rigid-rigid boundaries is made with those of an earlier work and good agreement is found. The study has limitations in the sense that thermophysical properties are calculated by using various quantities modelled for static condition.

***Keywords*—**Enclosures, free-free, rigid-rigid and rigid-free boundaries, Ginzburg-Landau model, Lorenz model.

I. Introduction

EFFORTS to have high thermally conducting cooling liquids and compact devices have been the endeavour of the engineers in the last few decades. Nanoliquids (base liquids+dilute concentration of 10-100 nm size nanoparticles) are a new kind of heat transfer liquids. The baseliquids commonly used are water, ethylene-glycol, engine oil, glycerine, lubricants, bio-fluids and polymer solutions. The nanoparticles used in nanoliquids are metals, oxides, carbides, nitrides and nonmetals.

Choi et al. [5], Masuda et al. [13], Eastman et al. [8] and Das et al. [7] were among the first to report increase in thermal conductivity of liquids due to addition of nanoparticles. To study the heat transfer phenomenon by suspending dilute concentration of nanoparticles in base liquid there are two approaches which have been adopted in the literature. Firstly the two-phase model ([3], [16]) that takes into account the role of fluid and solid phase in heat transfer process. The second one is the single-phase model ([12], [17]) where both the fluid phase and the solid phase are in thermal equilibrium state. In the absence of any experimental data in the literature on heat transport in nanoliquids, it remains to be an open problem as to whether the single-phase or the two-phase model is the best for studying Rayleigh-Bénard convection in nanoliquids. If the main interest is focused on the heat transfer process, then single-phase model is more convenient than the two-phase model. This statement is because of the superior characteristics of the nanoliquid which behave like a fluid rather than the conventional liquid-solid mixtures.

P. G. Siddheshwar and B. N. Veena are with the Department of Mathematics, Bangalore University, Bengaluru-560056, Karnataka, India (e-mail: mathdrpgs@gmail.com, mvymath@gmail.com).

Heat transfer in enclosure filled with nanoliquid has been studied widely in the past. Khanafer et al. [12] studied numerically natural convection problem in a differentially heated square cavity by considering the dispersion effect. Tiwari and Das [18] studied heat transfer in square cavity with lateral walls not being fixed. Further Rayleigh-Bénard convection with vertical boundary effects has been investigated by many using single-phase model ([12], [15], [6], [1], [11]).

In the present paper onset of convection and heat transport is studied using single-phase model for three different types of boundary conditions considering shallow, square and tall enclosures. The thermophysical properties are calculated using phenomenological laws [2] and mixture theory [10].

The main objective of the paper is to consider a simple model of nanoliquid and study the following:
(i) The effect of three different boundary combinations on onset and heat transfer.
(ii) Among shallow, square and tall ones which enclosure transports more heat.
(iii) Among the five-water based nanoliquids which nanoliquid transports more heat.

II. Nomenclature

Latin Symbols

a	ratio of thermal diffusivity
A	aspect ratio
b	width of enclosure
C_p	specific heat
$\vec{g}$	acceleration due to gravity $(0, 0, -g)$
h	height of enclosure
k	thermal conductivity
Nu	Nusselt number
p	pressure
Pr	Prandtl number
r	scaled Rayleigh number
$\vec{q}$	velocity vetor (u, w)
Ra	Rayleigh number
t	time
T	temperature
T_0	temperature at the lower boundary
u	horizontal velocity component

w	vertical velocity component
x	dimensional horizontal coordinate
X	non-dimensional horizontal coordinate
z	dimensional vertical coordinate
Z	non-dimensional vertical coordinate
Greek symbols	
α	thermal diffusivity
β	thermal expansion coefficient
χ	volume fraction
ΔT	temperature difference
μ	dynamic viscosity
μ_1	constant
μ_2	constant
∇^2	Laplacian operator $(\frac{\partial^2}{\partial x^2}+\frac{\partial^2}{\partial z^2})$
ψ	stream function
Ψ	non-dimensional stream function
ρ	actual density
τ	non-dimensional time
Θ	non-dimensional temperature
Subscripts	
b	basic state
bl	base liquid
c	critical
nl	nanoliquid
np	nanoparticle
Superscript	
FF	free-free
RF	rigid-free
RR	rigid-rigid
$'$	prime

III. Mathematical Formulation

Consider two-dimensional square, tall and shallow enclosures filled with nanoliquid as shown in Fig. 1. The horizontal walls are at a distance h. The upper and lower walls are maintained at constant temperatures T_0 and $T_0+\Delta T(\Delta T>0)$ respectively. The vertical walls are adiabatic and are at a distance b from each other. The Rayleigh-Bénard convection problem is assumed to be governed by single-phase model. The nanoliquid is taken to be Newtonian and incompressible. The nanoparticles are assumed to have a uniform size and spherical shape with identical smoothness (or roughness). Laminar regime of free convection is considered for investigation.

The governing conservation laws for studying the chosen problem are:

Conservation of Mass

$$\frac{\partial u}{\partial x}+\frac{\partial w}{\partial z}=0, \tag{1}$$

Conservation of Momentum

$$\rho_{nl}(T_0)\left[\frac{\partial u}{\partial t}+u\frac{\partial u}{\partial x}+w\frac{\partial u}{\partial z}\right]=-\frac{\partial p}{\partial x}+\mu_{nl}\nabla^2 u, \tag{2}$$

$$\rho_{nl}(T_0)\left[\frac{\partial w}{\partial t}+u\frac{\partial w}{\partial x}+w\frac{\partial w}{\partial z}\right]=-\frac{\partial p}{\partial z}+\mu_{nl}\nabla^2 w - \left[\rho_{nl}(T_0)-(\rho\beta)_{nl}(T-T_0)\right]g, \tag{3}$$

Conservation of Energy

$$\frac{\partial T}{\partial t}+u\frac{\partial T}{\partial x}+w\frac{\partial T}{\partial z}=\alpha_{nl}\nabla^2 T. \tag{4}$$

The thermophysical properties of nanoliquid are obtained as a function of the properties of base liquid and nanoparticles using phenomenological laws and mixture theory and are as documented below:

A. Phenomenological Laws

$$\frac{\mu_{nl}}{\mu_{bl}}=\frac{1}{(1-\chi)^{2.5}} \quad \text{(Brinkman model [2])}, \tag{5}$$

$$\frac{k_{nl}}{k_{bl}}=\frac{\left(\frac{k_{np}}{k_{bl}}+2\right)-2\chi\left(1-\frac{k_{np}}{k_{bl}}\right)}{\left(\frac{k_{np}}{k_{bl}}+2\right)+\chi\left(1-\frac{k_{np}}{k_{bl}}\right)} \tag{6}$$

(Hamilton-Crosser model [10]).

B. Mixture Theory

$$\left.\begin{aligned}\frac{\rho_{nl}}{\rho_{bl}}&=(1-\chi)+\chi\frac{\rho_{np}}{\rho_{bl}},\\ \frac{(\rho\beta)_{nl}}{(\rho\beta)_{bl}}&=(1-\chi)+\chi\frac{(\rho\beta)_{np}}{(\rho\beta)_{bl}},\\ \frac{(\rho C_p)_{nl}}{(\rho C_p)_{bl}}&=(1-\chi)+\chi\frac{(\rho C_p)_{np}}{(\rho C_p)_{bl}},\\ \alpha_{nl}&=\frac{k_{nl}}{(\rho C_p)_{nl}}\end{aligned}\right\}. \tag{7}$$

Temperature of nanoparticles is assumed to be constant on the horizontal boundaries and vertical boundaries are taken to be adiabatic. Hence the boundary conditions on T are:

$$\left.\begin{aligned}T=T_0+\Delta T \ \text{ at } z=-\frac{h}{2}\\ T=T_0 \text{ at } \ z=\frac{h}{2}\end{aligned}\right\}, -\frac{b}{2}<x<\frac{b}{2}, \tag{8}$$

$$\left.\frac{\partial T}{\partial x}=0 \ \text{ at } x=-\frac{b}{2},\frac{b}{2}\right\}, -\frac{h}{2}<z<\frac{h}{2}. \tag{9}$$

The three boundary conditions on velocity are mentioned a little later in the paper.

C. Basic State Solution

In the basic state the nanoliquid is assumed to be at rest and physical quantities vary along z-direction only and are given by

$$u=w=(0,0),\ p=p_b(z),\ T_b=T_b(z),\ \rho=\rho_b(z). \tag{10}$$

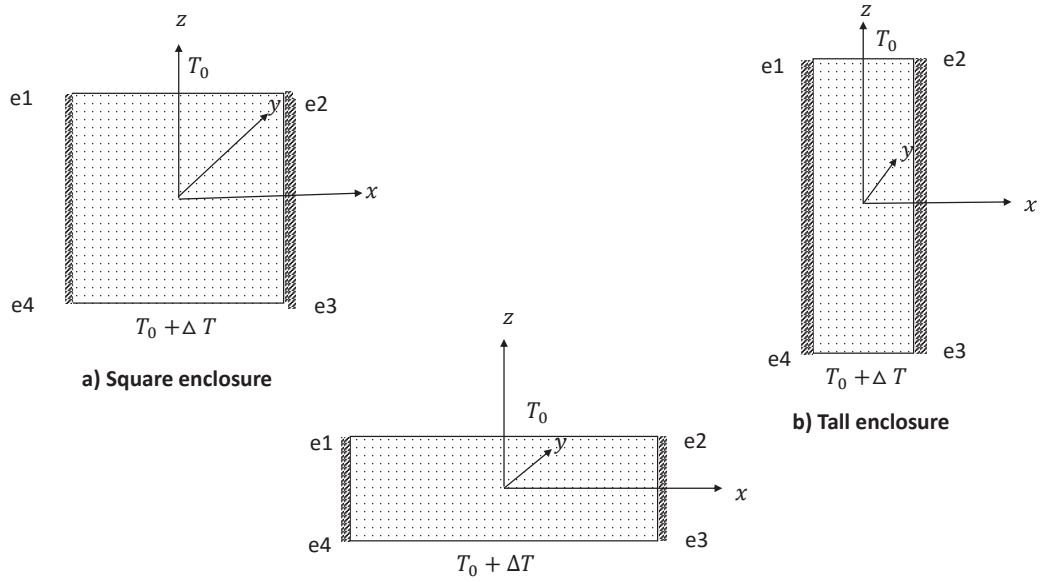

Fig. 1 Schematic representation of the flow configuration

The basic-state quantities satisfy the following equations:

$$\frac{\partial p_b}{\partial x} = 0, \tag{11}$$

$$-\frac{dp_b}{dz} = [\rho_{nl}(T_0) - (\rho\beta)_{nl}(T_b - T_0)]g, \tag{12}$$

$$\frac{d^2T_b}{dz^2} = 0. \tag{13}$$

The solution of (13), subject to temperature condition in (8) is:

$$T_b(z) = T_0 + \Delta T\left(\frac{1}{2} - \frac{z}{h}\right). \tag{14}$$

D. Perturbation State

On the quiescent basic state we superimpose perturbation in the form:

$$u = u',\ w = w',\ p = p_b + p',\ T = T_b + T',\ \rho = \rho_b + \rho'. \tag{15}$$

where the prime indicates a perturbed quantity and these quantities are functions of x, z and t.

Substituting the expression (15) by neglecting primes, using quiescent basic state solution, eliminating pressure terms between (2) and (3), and introducing stream function in the form:

$$u = \frac{\partial \psi}{\partial z},\ w = -\frac{\partial \psi}{\partial x}. \tag{16}$$

Equations (2)-(4) take the form:

$$\rho_{nl}(T_0)\left[\frac{\partial}{\partial t}(\nabla^2\psi) - \frac{\partial(\psi,\nabla^2\psi)}{\partial(x,z)}\right] = -(\rho\beta)_{nl}g\frac{\partial T}{\partial x} + \mu_{nl}\nabla^4\psi, \tag{17}$$

$$\frac{\partial T}{\partial t} + \frac{\Delta T}{h}\frac{\partial \psi}{\partial x} - \frac{\partial(\psi,T)}{\partial(x,z)} = \alpha_{nl}\nabla^2 T. \tag{18}$$

E. Non-Dimensionalization

Non-dimensionalizing (17)-(18) using the following definition

$$(X,Z) = \left(\frac{x}{b},\frac{z}{h}\right),\ \tau = \frac{t\alpha_{bl}}{h^2},\ \Psi = \frac{\psi}{\alpha_{bl}},\ \Theta = \frac{T}{\Delta T},$$
$$\nabla_A^2 = A^2\frac{\partial^2}{\partial X^2} + \frac{\partial^2}{\partial Z^2},$$

we get non-dimensional form of vorticity and heat transport equations as follows:

$$\frac{1}{Pr_{nl}}\frac{\partial}{\partial \tau}(\nabla_A^2\Psi) = -a^2 Ra_{nl}A^4\frac{\partial \Theta}{\partial X} + a\nabla_A^4\Psi + \frac{1}{Pr_{nl}}A\frac{\partial(\Psi,\nabla_A^2\Psi)}{\partial(X,Z)}, \tag{19}$$

$$\frac{\partial \Theta}{\partial \tau} = -A\frac{\partial \Psi}{\partial X} + A\frac{\partial(\Psi,\Theta)}{\partial(X,Z)} + a\nabla_A^2\Theta. \tag{20}$$

The non-dimensional parameters appearing in (19) and (20) are,

$$\left.\begin{aligned} Pr_{nl} &= \frac{\mu_{nl}}{\rho_{nl}(T_0)\alpha_{nl}}(\text{Prandtl number}),\\ A &= \frac{h}{b}(\text{Aspect ratio}),\\ a &= \frac{\alpha_{nl}}{\alpha_{bl}}(\text{Thermal diffusivity ratio}),\\ Ra_{nl} &= \frac{(\rho\beta)_{nl}g\Delta T b^3}{\mu_{nl}\alpha_{nl}}(\text{Rayleigh number}) \end{aligned}\right\}. \tag{21}$$

F. Boundary Conditions

To solve (19) and (20) we consider three sets of boundary conditions:

Case (i): Free-free isothermal horizontal (FFIH) boundaries and free-free adiabatic vertical (FFAV) boundaries

$$\left.\begin{aligned}\Psi = \frac{\partial^2\Psi}{\partial Z^2} = \Theta = 0 \;\; at \;\; Z = -\frac{1}{2}, \frac{1}{2}\,, \;\; \frac{-1}{2} < X < \frac{1}{2} \\ \Psi = \frac{\partial^2\Psi}{\partial X^2} = \frac{\partial\Theta}{\partial X} = 0 \; at \; X = -\frac{1}{2}, \frac{1}{2}\,, \;\; \frac{-1}{2} < Z < \frac{1}{2}\end{aligned}\right\}. \tag{22}$$

Case (ii): Rigid-rigid isothermal horizontal (RRIH) boundaries and rigid-rigid adibatic vertical (RRAV) boundaries

$$\left.\begin{aligned}\Psi = \frac{\partial\Psi}{\partial Z} = \Theta = 0 \;\; at \;\; Z = -\frac{1}{2}, \frac{1}{2}\,, \;\; \frac{-1}{2} < X < \frac{1}{2} \\ \Psi = \frac{\partial\Psi}{\partial X} = \frac{\partial\Theta}{\partial X} = 0 \;\; at \;\; X = -\frac{1}{2}, \frac{1}{2}\,, \;\; \frac{-1}{2} < Z < \frac{1}{2}\end{aligned}\right\}. \tag{23}$$

Case (iii): Rigid-free isothermal horizontal (RFIH) boundaries and rigid-rigid adiabatic vertical (RRAV) boundaries

$$\left.\begin{aligned}\Psi = \frac{\partial\Psi}{\partial Z} = \Theta = 0 \;\; at \;\; Z = -\frac{1}{2}\,, \;\; \frac{-1}{2} < X < \frac{1}{2} \\ \Psi = \frac{\partial^2\Psi}{\partial Z^2} = \Theta = 0 \;\; at \;\; Z = \frac{1}{2}\,, \;\; \frac{-1}{2} < X < \frac{1}{2} \\ \Psi = \frac{\partial\Psi}{\partial X} = \frac{\partial\Theta}{\partial X} = 0 \;\; at \;\; X = -\frac{1}{2}, \frac{1}{2}\,, \;\; \frac{-1}{2} < Z < \frac{1}{2}\end{aligned}\right\}. \tag{24}$$

G. Stability Analysis

Since principle of exchange of stabilities (PES) is valid we consider only stationary convection in our study. This is done by considering the linear and steady-state version of (19) and (20) and their normal mode solutions are assumed to be as follows:

Case (i)

$$\Psi(X,Z) = \Psi_0 \sin\left(\pi X + \frac{\pi}{2}\right)\sin\left(\pi Z + \frac{\pi}{2}\right), \tag{25}$$

$$\Theta(X,Z) = \Theta_0 \cos\left(\pi X + \frac{\pi}{2}\right)\sin\left(\pi Z + \frac{\pi}{2}\right), \tag{26}$$

where Ψ_0, Θ_0 are infinitesimal amplitudes of the stream function and temperature. The solutions (25) and (26) satisfy the boundary conditions in (22). Substituting (25) and (26) in linear and steady-state version of (19) and (20) and following classical procedure, we obtain the expression for Ra_{nlc}^{FF} (critical Rayleigh number for free-free boundaries) in the form:

$$Ra_{nlc}^{FF} = \frac{\delta_A^6}{\pi^2 A^5}, \tag{27}$$

where $\delta_A^2 = \pi^2(A^2+1)$.

Case (ii)

$$\Psi(X,Z) = \Psi_0 C_{fe}(X) C_{fe}(Z), \tag{28}$$

$$\Theta(X,Z) = \Theta_0 \cos\left(\pi X + \frac{\pi}{2}\right)\sin\left(\pi Z + \frac{\pi}{2}\right), \tag{29}$$

where $C_{fe}(X)$ and $C_{fe}(Z)$ are Chandrasekar's even function ([4], [14]). The solution in (28) and (29) satisfy the boundary conditions in (23). Following the procedure of case (i), we obtain the expression for Ra_{nlc}^{RR} (critical Rayleigh number for rigid-rigid boundaries) in the form:

$$Ra_{nlc}^{RR} = \frac{\delta_A^2}{4A^3P_2^2}\left[\frac{P_3(1+A^4)}{A^2} + P_4\right], \tag{30}$$

where

$$P_2 = \frac{16\pi^3\mu_1^4}{(\pi^4-\mu_1^4)^2}, \;\; P_3 = \frac{\mu_1^2}{16}P_6P_7^2,$$

$$P_4 = \frac{\mu_1^2}{8}P_6P_8^2, \;\; P_6 = \sec^4[\frac{\mu_1}{2}]\,\mathrm{sech}^4[\frac{\mu_1}{2}],$$

$$P_7 = 2\sin[\mu_1]\cosh^2[\frac{\mu_1}{2}] + 2\sinh[\mu_1]\cos^2[\frac{\mu_1}{2}] - \mu_1(2+\cos[\mu_1]+\cosh[\mu_1]),$$

$$P_8 = 2\sin[\mu_1]\cosh^2[\frac{\mu_1}{2}] - 2\sinh[\mu_1]\cos^2[\frac{\mu_1}{2}] - \mu_1(\cos[\mu_1]-\cosh[\mu_1]),$$

$$\mu_1 = 4.73004074.$$

Case (iii)

$$\Psi(X,Z) = \Psi_0 C_{fo}(X) C_{fo}(Z), \tag{31}$$

$$\Theta(X,Z) = \Theta_0 \cos\left(2\pi X + \pi\right)\sin\left(2\pi Z + \pi\right), \tag{32}$$

where $C_{fo}(X)$ and $C_{fo}(Z)$ are Chandrashekar odd functions ([4], [14]). The solution in (31) and (32) satisfy the boundary conditions in (23). Following the procedure of case (i), and dividing the so obtained critical Rayleigh number by 16, as explained by Chandrasekhar [4], we get

$$Ra_{nlc}^{RF} = \frac{\delta_A^2}{16A^3E_2^2}\left[\frac{E_3(1+A^4)}{A^2} - E_4\right], \tag{33}$$

where

$$E_2 = \frac{128\pi^3\mu_2^4}{(-16\pi^4-\mu_2^4)^2}, \;\; E_3 = \frac{\mu_2^2}{16}E_6E_7^2,$$

$$E_4 = -\frac{\mu_2^2}{8}E_6E_8^2, \;\; E_6 = \csc^4[\frac{\mu_2}{2}]\,\mathrm{csch}^4[\frac{\mu_2}{2}],$$

$$E_7 = -2\sinh[\mu_2]\sinh^2[\frac{\mu_2}{2}] + 2\sin[\mu_2]\sinh^2[\frac{\mu_2}{2}] + \mu_2(-2+\cos[\mu_2]+\cosh[\mu_2]),$$

$$E_8 = 2\sin[\mu_2]\sinh^2[\frac{\mu_2}{2}] + 2\sinh[\mu_2]\sin^2[\frac{\mu_2}{2}] + \mu_2(\cos[\mu_2]-\cosh[\mu_2]),$$

$$\mu_2 = 7.85320.$$

The linear theory predicts only the onset of convection and does not give any information about heat transport. In order to study heat transport we need to perform a nonlinear stability analysis to find the effect of various parameters on finite-amplitude convection and thereby on heat transport.

H. Local Nonlinear Stability Analysis

In nonlinearity the temperature field is distorted by the interaction of Ψ and Θ. A minimal double Fourier series which describes the unsteady finite-amplitude convection is chosen for all three cases and substituting these into (19) and (20) we get generalized tri-modal Lorenz model which will be discussed later.

Case (i)

$$\Psi(X,Z,\tau)=\frac{\sqrt{2}\delta_A^2 a}{A\pi^2}U_1(\tau)\sin\left(\pi X+\frac{\pi}{2}\right)\sin\left(\pi Z+\frac{\pi}{2}\right), \tag{34}$$

$$\Theta(X,Z,\tau)=-\frac{\sqrt{2}}{r_1\pi}V_1(\tau)\cos\left(\pi X+\frac{\pi}{2}\right)\sin\left(\pi Z+\frac{\pi}{2}\right) -\frac{1}{r_1\pi}W_1(\tau)\sin\left(2\pi Z+\pi\right), \tag{35}$$

where

$$\delta_A^2=\pi^2(A^2+1),\ r_1=\frac{Ra_{nlm}^{FF}}{Ra_{nlc}^{FF}}.$$

Case (ii)

$$\Psi(X,Z,\tau)=\frac{\delta_A^2 a}{2\sqrt{2}AP_5}U_2(\tau)C_{fe}(X)C_{fe}(Z), \tag{36}$$

$$\Theta(X,Z,\tau)=-\frac{\sqrt{2}P_2}{r_2P_5}V_2(\tau)\cos\left(\pi X+\frac{\pi}{2}\right)\sin\left(\pi Z+\frac{\pi}{2}\right) -\frac{P_2}{r_2P_5}W_2(\tau)\sin\left(2\pi Z+\pi\right), \tag{37}$$

where

$$\delta_A^2=\pi^2(A^2+1),\ \ P_5=\frac{32\pi^3\mu_1^4(39\pi^4+\mu_1^4)}{(\pi^4-\mu_1^4)^2(81\pi^4-\mu_1^4)},$$
$$r_2=\frac{Ra_{nlm}^{RR}}{Ra_{nlc}^{RR}}.$$

Case (iii)

$$\Psi(X,Z,\tau)=\frac{\sqrt{2}\delta_A^2 a}{AE_5}U_3(\tau)C_{fo}(X)C_{fo}(Z), \tag{38}$$

$$\Theta(X,Z,\tau)=\frac{-\sqrt{2}E_2}{r_3E_5}V_3(\tau)\cos\left(2\pi X+\pi\right)\sin\left(2\pi Z+\pi\right) -\frac{E_2}{r_3E_5}W_3(\tau)\sin\left(4\pi Z+2\pi\right)] \tag{39}$$

where

$$\delta_A^2=\pi^2(A^2+1),\ \ E_5=\frac{512\pi^4\mu_2^4(624\pi^4+\mu_2^4)}{(1296\pi^4-\mu_2^4)(-16\pi^4+\mu_2^4)^2},$$
$$r_3=\frac{Ra_{nlm}^{RF}}{Ra_{nlc}^{RF}},$$

where $U_i,\ \ Vi$ and W_i are the amplitudes that are to be determined. On substituting the eigen functions of the above three cases in (19) and (20) and adopting orthogonalization procedure of the Galerkin expansion, we obtain the analytically intractable nonlinear autonomous system of differential equations called "Lorenz model".

$$\frac{dU_i}{d\tau_i}=\frac{Pr_{nl}}{Q_i}a[V_i-U_i], \tag{40}$$

$$\frac{dV_i}{d\tau_i}=a[r_iU_i-V_i-U_iW_i], \tag{41}$$

$$\frac{dW_i}{d\tau_i}=a[U_iV_i-b_iW_i]. \tag{42}$$

In the Lorenz equations (40)-(42), i=1, i=2, and i=3 correspond respectively to case (i), case (ii) and case (iii).

Case (i)

$$\tau_1=\delta_A^2\tau,\ Q_1=1,\ b_1=\frac{4\pi^2}{\delta_A^2}.$$

Case (ii)

$$\tau_2=\delta_A^2\tau,\ Q_2=-\frac{P_1\delta_A^6}{4\pi^2A^5Ra_{nlc}^{RR}P_2^2},$$
$$P_1=\frac{1}{16}P_6P_7P_8,\ b_2=\frac{4\pi^2}{\delta_A^2}.$$

Case (iii)

$$\tau_3=4\delta_A^2\tau,\ Q_3=-\frac{4(A^2+1)E_1\delta_A^4}{A^5Ra_{nlc}^{RF}E_2^2},$$
$$E_1=\frac{1}{16}E_6E_7E_8,\ b_3=\frac{4\pi^2}{\delta_A^2}.$$

All other quantities are as defined earlier.

I. Multiscale Method

From regular perturbation expansion, we have the following:

$$\left.\begin{aligned}U_i&=\epsilon U_{i1}+\epsilon^2U_{i2}+\epsilon^3U_{i3}+.....,\\V_i&=\epsilon V_{i1}+\epsilon^2V_{i2}+\epsilon^3V_{i3}+.....,\\W_i&=\epsilon W_{i1}+\epsilon^2W_{i2}+\epsilon^3W_{i3}+.....,\\r_i&=r_{i0}+\epsilon^2r_{i2}+.....\end{aligned}\right\}, \tag{43}$$

where r_{i0} is the critical Rayleigh number (scaled). We now use the following symbols for the matrices to be obtained by regular perturbation method.

$$M_{i1}=[U_i\ \ V_i\ \ W_i]^T\ \text{ and }\ L=\begin{pmatrix}-a & a & 0\\ ar_{i0} & -a & 0\\ 0 & 0 & -ab_i\end{pmatrix}. \tag{44}$$

Substituting (43) in (40)-(42) and using the time variation only at the slow time scale which is taken to be $\tau=\epsilon^2\tau^*$ and on comparing the like powers of ϵ on both sides of the resulting equations, we get the following equations at various orders.

First-order system

$$L\ M_{i1}=[0\ \ 0\ \ 0]^T. \tag{45}$$

Second-order system

$$L\ M_{i2} = [R_{21}\ R_{22}\ R_{23}]^T. \tag{46}$$

where

$$R_{21} = 0,\ R_{22} = -a\ r_{i1}U_i,\ R_{23} = -a\ U_i^2 r_{i0}.$$

Third-order system

$$L\ M_{i3} = [R_{31}\ R_{32}\ R_{33}]^T, \tag{47}$$

where

$$\left.\begin{aligned} R_{31} &= \frac{Q_i}{Pr_{nl}}\frac{dU_i}{d\tau^*} \\ R_{32} &= r_{i0}\frac{dU_i}{d\tau^*} - ar_{i2}U_i + ar_{i0}\frac{U_i^3}{b_i} \\ R_{33} &= -2aU_i r_{i0}U_{0i} \end{aligned}\right\}. \tag{48}$$

The solution of first-order and second-order systems are given by

$$[U_{i1}\ \ V_{i1}\ \ W_{i1}]^T = [U_i\ \ r_{i0}U_i\ \ 0]^T,$$
$$[U_{i2}\ \ V_{i2}\ \ W_{i2}]^T = [U_i\ \ r_{i0}U_i\ \ \frac{U_i^2}{b_i}r_{i0}]^T.$$

We are not interested in the solution of the third-order system. However, for the purpose of determining the amplitude it is sufficient to consider the Fredholm solvability condition which for the present problem is:

$$\begin{pmatrix} \widehat{U}_{i1} \\ \widehat{V}_{i1} \\ \widehat{W}_{i1} \end{pmatrix} \begin{pmatrix} R_{31} & R_{32} & R_{33} \end{pmatrix} = \begin{pmatrix} 0 \\ 0 \\ 0 \end{pmatrix}. \tag{49}$$

where $[\widehat{U}_{i1}\quad \widehat{V}_{i1}\quad \widehat{W}_{i1}]$ are the solution of the adjoint of first-order system.

Simplifying the solvability condition, we get Ginzburg-Landau equation as follows:

$$\frac{dU_i(\tau^*)}{d\tau^*} = F_{i1}U_i(\tau^*) - F_{i2}U_i^3(\tau^*), \tag{50}$$

where

$$F_{i1} = \left[\frac{aPr_{nl}}{Q_i + Pr_{nl}}\right],\ \ F_{i2} = \left[\frac{aPr_{nl}}{b_i[Q_i + Pr_{nl}]}\right].$$

Solving (50) we get amplitude in the form

$$U_i^2(\tau^*) = \frac{F_{i1}A_0^2}{F_{i2}A_0^2 + (F_{i1} - F_{i2}A_0^2)e^{-2F_{i1}\tau^*}} \tag{51}$$

where $A_0 = 1$. In calculations we have assumed $r_{i0} = r_{i2} = 1$ for simplification.

Case(i)

$$\frac{dU_1(\tau^*)}{d\tau^*} = F_{11}U_1(\tau^*) - F_{12}U_1^3(\tau^*), \tag{52}$$

where

$$F_{11} = \left[\frac{aPr_{nl}}{Q_1 + Pr_{nl}}\right],\ \ F_{12} = \left[\frac{aPr_{nl}}{b_1[Q_1 + Pr_{nl}]}\right].$$

Solving (52) we get amplitude in the form

$$U_1^2(\tau^*) = \frac{F_{11}A_0^2}{F_{12}A_0^2 + (F_{11} - F_{12}A_0^2)e^{-2F_{11}\tau^*}}. \tag{53}$$

Case(ii)

$$\frac{dU_2(\tau^*)}{d\tau^*} = F_{21}U_2(\tau^*) - F_{22}U_2^3(\tau^*), \tag{54}$$

where

$$F_{21} = \left[\frac{aPr_{nl}}{Q_2 + Pr_{nl}}\right],\ \ F_{22} = \left[\frac{aPr_{nl}}{b_2[Q_2 + Pr_{nl}]}\right].$$

Solving (54) we get amplitude in the form

$$U_2^2(\tau^*) = \frac{F_{21}A_0^2}{F_{22}A_0^2 + (F_{21} - F_{22}A_0^2)e^{-2F_{21}\tau^*}}. \tag{55}$$

Case(iii)

$$\frac{dU_3(\tau^*)}{d\tau^*} = F_{31}U_3(\tau^*) - F_{32}U_3^3(\tau^*), \tag{56}$$

where

$$F_{31} = \left[\frac{aPr_{nl}}{Q_3 + Pr_{nl}}\right],\ \ F_{32} = \left[\frac{aPr_{nl}}{b_3[Q_3 + Pr_{nl}]}\right].$$

Solving (56) we get amplitude in the form

$$U_3^2(\tau^*) = \frac{F_{31}A_0^2}{F_{32}A_0^2 + (F_{31} - F_{32}A_0^2)e^{-2F_{31}\tau^*}}. \tag{57}$$

In the next section we study the heat transport in terms of the Nusselt number at the lower boundary.

J. Estimation of Enhanced Heat Transport in Nanoliquids at Lower Boundary

$$Nu_{nl} = \frac{\text{Heat transport by (conduction+convection)}}{\text{Heat transport by conduction}}. \tag{58}$$

From Fourier laws, we know that

$$\text{Heat transport by conduction} = \left[-k_{bl}\int_{-\frac{1}{2}}^{\frac{1}{2}} \frac{d\Theta_b}{dZ}dX\right]_{Z=-\frac{1}{2}}, \tag{59}$$

$$\text{Heat transport by convection} = \left[-k_{nl}\int_{-\frac{1}{2}}^{\frac{1}{2}} \frac{\partial\Theta}{\partial Z}dX\right]_{Z=-\frac{1}{2}}. \tag{60}$$

$$Nu_{nl} = 1 + \frac{k_{nl}}{k_{bl}}\left[\frac{-\int_{-\frac{1}{2}}^{\frac{1}{2}} \frac{\partial\Theta}{\partial Z}dX}{-\int_{-\frac{1}{2}}^{\frac{1}{2}} \frac{d\Theta_b}{dZ}dX}\right]_{Z=-\frac{1}{2}}. \tag{61}$$

Case(i)

$$Nu_{nl}^{FF} = 1 + 2\frac{k_{nl}}{k_{bl}}\frac{U_1^2}{b_1}\left(1 - \frac{1}{r_1}\right). \tag{62}$$

Case(ii)

$$Nu_{nl}^{RR} = 1 + 2\pi \frac{P_2}{P_5} \frac{k_{nl}}{k_{bl}} \frac{U_2^2}{b_2} \left(1 - \frac{1}{r_2}\right). \tag{63}$$

Case(iii)

$$Nu_{nl}^{RF} = 1 + 4\pi \frac{E_2}{E_5} \frac{k_{nl}}{k_{bl}} \frac{U_3^2}{b_3} \left(1 - \frac{1}{r_3}\right). \tag{64}$$

IV. Conclusion

Rayleigh-Bénard convection in nanoliquid filled enclosure is studied for three different boundary combinations namely FF, RF and RR by considering water-copper, water-copperoxide, water-silver, water-alumina and water-titania nanoliquids. Thermophysical properties of baseliquids, nanoparticles, and nanoliquids are all collected from literature ([16], [17]) and tabulated in Tables I and II. In plotting graphs water-copper has been taken as representative nanoliquid and similar observation to that of water-copper is noticed in other nanoliquids.

From linear stability ananlyses for the three boundary combinations considered for A=1 and χ=0.06, the following critical Rayleigh numbers have been obtained:

$$Ra_{nlc}^{FF} = 779.273 < Ra_{nlc}^{RF} = 1629.41 < Ra_{nlc}^{RR} = 2756.26.$$

From Table III it is clear that onset of convection is advanced in tall enclosure compared to square enclosure and shallow enclosure respectively for FF, RF, and RR boundaries.
It is further found that Ra_{nl}, for all three boundaries, can be rewritten as follows:

$$Ra_{nl} = F\ Ra_{bl},\ F = \frac{(\rho\beta)_{nl}}{(\rho\beta)_{bl}} \frac{\mu_{bl}}{\mu_{nl}} \frac{\alpha_{bl}}{\alpha_{nl}}. \tag{65}$$

We found that $F < 1$ for all water-based nanoliquids when the values in Tables I and II are used in (65). In the absence of nanoparticles $F = 1$. This implies that $Ra_{nl} < Ra_{bl}$. This explains advanced onset of convection and hence enhanced heat transfer in nanoliquids.

Nusselt number increases with increase in Rayleigh number for FF, RF and RR boundaries as shown in Tables IV-VI for different nanoliquids and the same is also observed in the graphs. It is further observed that among the five water-based nanoliquids considered water-copper transports more heat compared to other nanoliquids for FF boundaries whereas water-silver transports more heat for RF and RR boundaries. This observed phenomenon is due to high thermal conductivities of copper and silver nanoparticles. Water-titania transports least heat for all three boundaries because of its low thermal conductivity.

The Nusselt number results of the present problem for RR boundaries are compared with the results of Elhajjar et al. [9] for $Ra_{nlc}^{RR} = 5000$ and $\chi = 0.08$ which is in good agreement for rectangular enclosure and this is shown in Table VII. The mismatch in results on the effect of χ on Nu_{nl} between our results and Elhajjar et al. [9] is due to the wrong definition of specific heat and thermal expansion coefficient of nanoliquid used in Elhajjar et al. [9] paper. In our paper, we have obtained thermodynamically correct result by using the following definition:

$$(C_p)_{nl} = \frac{(1-\chi)(\rho C_p)_{bl} + \chi(\rho C_p)_{np}}{(1-\chi)\rho_{bl} + \chi\rho_{np}}, \tag{66}$$

$$\beta_{nl} = \frac{(1-\chi)(\rho\beta)_{bl} + \chi(\rho\beta)_{np}}{(1-\chi)\rho_{bl} + \chi\rho_{np}}. \tag{67}$$

From Figs. 2-10 it is clear that Nusselt number increases with the increase in aspect ratio, critical Rayleigh number and volume fraction for FF, RF and RR boundaries. Further from graphs for different aspect ratio it is clear that the model is valid for $A \geq 0.85$, below which the convection phenomenon in enclosure problem becomes multi-cellular Rayleigh-Bénard convection. Further, from these graphs it is very much clear that FF boundaries transports more heat compared to RF and RR boundaries respectively. The same can be observed in Fig. 11. From Table VIII increment in heat transfer is found to be in the range 4.8572%-11.0224%, 4.4027%-10.7487%, 3.8768%-10.2469% in presence of nanoparticles, for different aspect ratio, for FF, RF and RR boundaries respectively.

In general we can conclude that the presence of nanoparticles advances onset of convection and hence enhances heat transport which is true for dilute concentration of nanoparticles.

TABLE I
Thermophysical Properties of Base Liquid and Nanoparticles at 300^0K

Quantity	μ	ρ	k	$\beta \times 10^5$	C_p
water	0.00089	997	0.613	21	4179
copper	-	8933	401	1.67	531.8
copper-oxide	-	6320	76.5	1.8	235
silver	-	10500	429	1.89	235
alumina	-	3970	40	0.85	765
titania	-	4250	8.9538	0.9	686.2

TABLE II
Thermophysical Properties of Nanoliquid at 300^0K

Nanoliquids	μ_{nl}	ρ_{nl}	k_{nl}	$\alpha_{nl} \times 10^7$
water-copper	0.00104	1473.25	0.72981	1.77001
water-copper oxide	0.00104	1316.47	0.72743	1.76625
water-silver	0.00104	1567.27	0.72985	1.79548
water-alumina	0.00104	1175.47	0.72483	1.76827
water-titania	0.00104	1192.27	0.70808	1.73047

TABLE III
Comparision of Critical Rayleigh Number for FF, RF and RR Boundaries for $\chi = 0.06$

Quantity	Ra_{nlc}^{FF}	Ra_{nlc}^{RF}	Ra_{nlc}^{RR}
A=0.8	1311.2400	2779.2400	4757.5100
A=1	0779.2730	1629.4100	2756.2600
A=1.2	0568. 6730	1200.0400	2046.4100

TABLE IV
VALUES OF NANOLIQUID NUSSELT NUMBER, Nu_{nl}^{FF}, FOR $\chi = 0.06$, $A_0 = 1$, $\tau^* = 2$ AND $Ra_{nlc}^{FF} = 779.2730$, WITH $Nu_{bl}^{FF} = 1.9687$ FOR $Ra_{nl}^{FF} = 2Ra_{nlc}^{FF}$ AND $Nu_{bl}^{FF} = 2.2916$ FOR $Ra_{nl}^{FF} = 3Ra_{nlc}^{FF}$ FOR FF BOUNDARIES

Nanoliquids	$2 \times Ra_{nlc}^{FF}$	% increase	$3 \times Ra_{nlc}^{FF}$	% increase
water-copper	2.1656	10.0015	2.5542	11.4592
water-copper oxide	2.1636	9.8999	2.5515	11.3414
water-silver	2.1656	10.0015	2.5541	11.4548
water-alumina	2.1612	9.7780	2.5483	11.2017
water-titania	2.1327	8.3303	2.5103	9.5435

TABLE V
VALUES OF Nu_{nl}^{RF}, FOR $\chi = 0.06$, $A_0 = 1$, $\tau^* = 2$ AND $Ra_{nlc}^{RF} = 1629.4100$, WITH $Nu_{bl}^{RF} = 1.9214$ FOR $Ra_{nl}^{RF} = 2Ra_{nlc}^{RF}$ AND $Nu_{bl}^{RF} = 2.2285$ FOR $Ra_{nl}^{RF} = 3Ra_{nlc}^{RF}$ FOR RF BOUNDARIES

Nanoliquids	$2 \times Ra_{nlc}^{RF}$	% increase	$3 \times Ra_{nlc}^{RF}$	% increase
water-copper	2.1088	9.7533	2.4785	11.2183
water-copper oxide	2.1064	9.6283	2.4752	11.0702
water-silver	2.1090	9.7637	2.4787	11.2272
water-alumina	2.1036	9.4826	2.4715	10.9041
water-titania	2.0767	8.0826	2.4356	9.2932

TABLE VI
VALUES OF Nu_{nl}^{RR}, FOR $\chi = 0.06$, $A_0 = 1$, $\tau^* = 2$ AND $Ra_{nlc}^{RR} = 2756.2600$, WITH $Nu_{bl}^{RR} = 1.8399$ FOR $Ra_{nl}^{RR} = 2Ra_{nlc}^{RR}$ AND $Nu_{bl}^{RR} = 2.1199$ FOR $Ra_{nl}^{RR} = 3Ra_{nlc}^{RR}$ FOR RR BOUNDARIES

Nanoliquids	$2 \times Ra_{nlc}^{RR}$	% increase	$3 \times Ra_{nlc}^{R}$	% increase
water-copper	2.0107	9.2831	2.3476	10.7410
water-copper oxide	2.0077	9.1200	2.3437	10.5571
water-silver	2.0111	9.3048	2.3482	10.7693
water-alumina	2.0046	8.9515	2.3395	10.3589
water-titania	1.9803	7.6308	2.3071	8.8306

TABLE VII
COMPARISION OF THE PRESENT PROBLEM WITH THAT OF ELHAJJAR ET AL. [9] FOR RR BOUNDARIES

Quantity	Nu_{nl}^{RR}	Nu_{bl}^{RR}	% increase
A=0.81	1.1743	1.1359	3.3805
A=0.83	1.3033	1.2365	5.4023
A=0.85	1.4174	1.3257	6.9171
A=0.87	1.5187	1.4050	8.0925
A=0.89	1.6089	1.4757	9.0262

TABLE VIII
COMPARISON OF NANOLIQUID WITH $\chi = 0.06$ AND BASE LIQUID NUSSELT NUMBER, FOR $A_0 = 1$, $\tau^* = 2$ FOR FF, RF AND RR BOUNDARIES WITH DIFFERENT ASPECT RATIO

Quantity	$Ra_{nlc}^{FF} = 2Ra_{nlc}^{FF}$		$Ra_{nlc}^{RF} = 2Ra_{nlc}^{RF}$		$Ra_{nlc}^{RR} = 2Ra_{nlc}^{RR}$	
	Nu_{nl}^{FF}	Nu_{bl}^{FF}	Nu_{nl}^{RF}	Nu_{bl}^{RF}	Nu_{nl}^{RR}	Nu_{bl}^{RR}
A=0.8	1.3665	1.3032	1.3232	1.2674	1.2754	1.2278
% increase	4.8572		4.4027		3.8768	
A=1	2.1656	1.9687	2.1088	1.9214	2.0107	1.8399
% increase	10.0015		9.7533		9.2831	
A=1.2	2.4919	2.2445	2.4110	2.1770	2.2766	2.0650
% increase	11.0224		10.7487		10.2469	

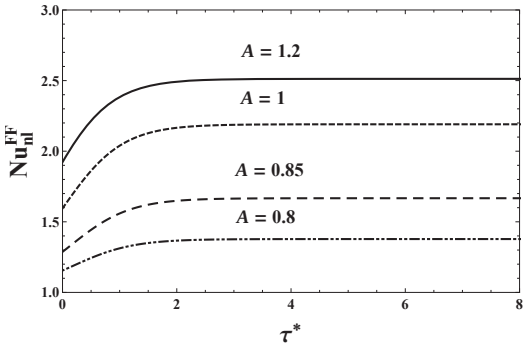

Fig. 2 Variation of nanoliquid Nusselt number, Nu_{nl} with time, τ^* for different aspect ratio, A with volume fraction, $\chi = 0.06$ and Rayleigh number, $Ra = 2Ra_{nlc}$ for water-copper nanoliquid for FF boundaries

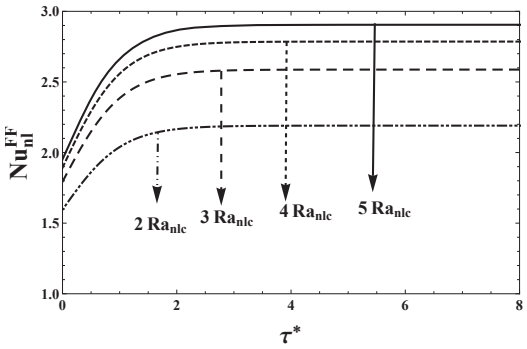

Fig. 3 Variation of Nu_{nl} with τ^* for different Ra_{nl} with $\chi = 0.06$ and A=1 for water-copper nanoliquid for FF boundaries

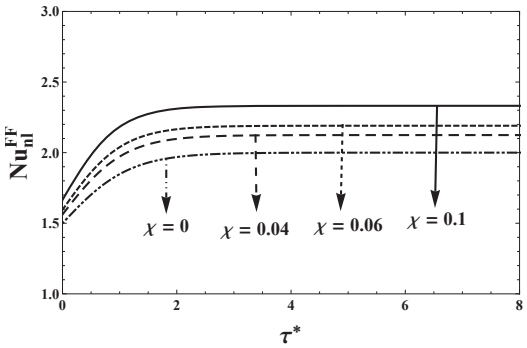

Fig. 4 Variation of Nu_{nl} with τ^* for different χ with $Ra = 2Ra_{nlc}$ and A=1 for water-copper nanoliquid for FF boundaries

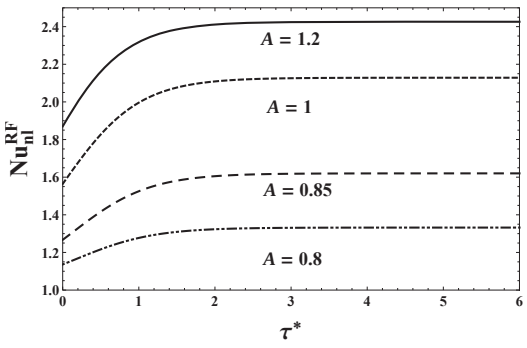

Fig. 5 Variation of Nu_{nl} with τ^* for different A with $\chi = 0.06$ and $Ra = 2Ra_{nlc}$ for water-copper nanoliquid for RF boundaries

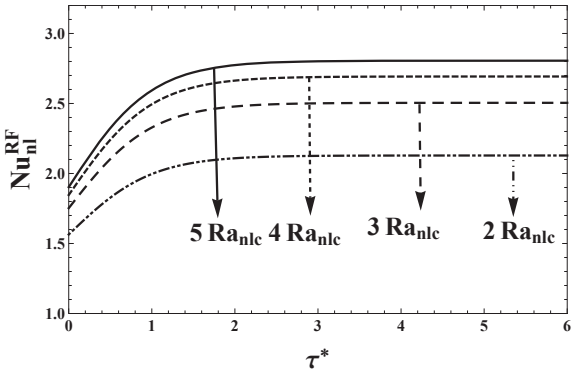

Fig. 6 Variation of Nu_{nl} with τ^* for different Ra_{nl} with $\chi = 0.06$ and A=1 for water-copper nanoliquid for RF boundaries

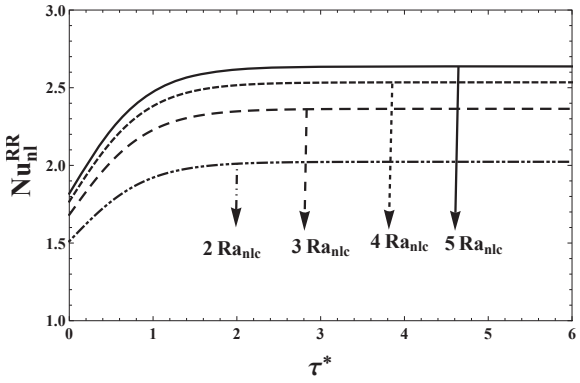

Fig. 9 Variation of Nu_{nl} with τ^* for different Ra_{nl} with $\chi = 0.06$ and A=1 for water-copper nanoliquid for RR boundaries

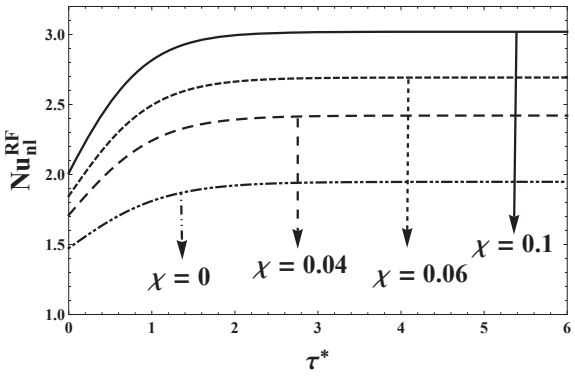

Fig. 7 Variation of Nu_{nl} with τ^* for different χ with $Ra = 2Ra_{nlc}$ and A=1 for water-copper nanoliquid for RF boundaries.

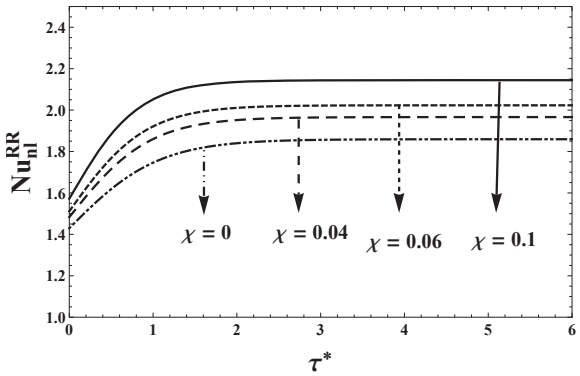

Fig. 10 Variation of Nu_{nl} with τ^* for different χ with $Ra = 2Ra_{nlc}$ and A=1 for water-copper nanoliquid for RR boundaries

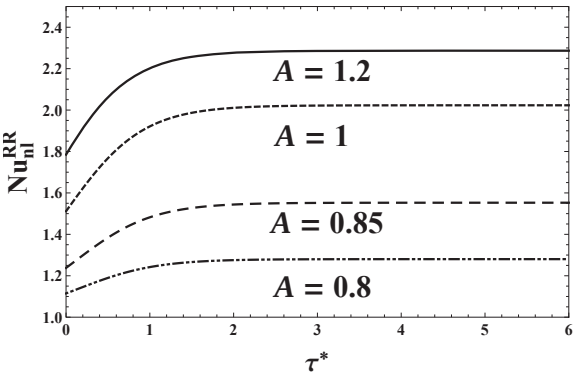

Fig. 8 Variation of Nu_{nl} with τ^* for different A with $\chi = 0.06$ and $Ra = 2Ra_{nlc}$ for water-copper nanoliquid for RR boundaries

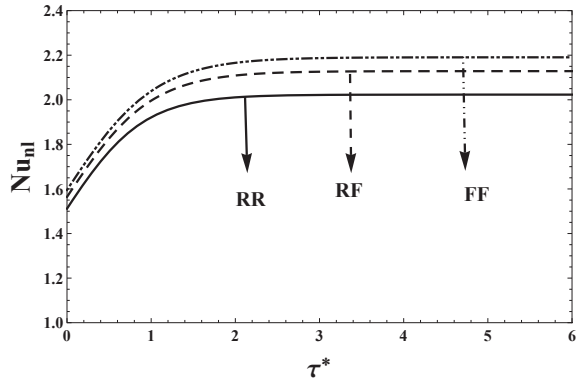

Fig. 11 Variation of Nu_{nl} with τ^* for FF, RF and RR boundary combinations

ACKNOWLEDGMENT

One of the authors(VBN) would like to thank the University Grants Commission, Government of India, for awarding her the "National Fellowship for Higher Education" to carry out her research. The authors thank the Bangalore university for encouragement and support.

REFERENCES

[1] E. Abu-Nada and A. J. Chamkha, *Effect of nanofluid variable properties on natural convection in enclosures filled with a CuO-EG water nanofluid*, Int. J. Therm. Sci., 49, pp. 2339-2352, 2010.
[2] H. C. Brinkman, *The viscosity of concentrated suspensions and solutions*, J. Chem. Phys., 20, pp. 571-571, 1952.
[3] J. Buongiorno, *Convective transport in nanofluids*, ASME J. Heat Trans., 128, pp. 240-250, 2006.
[4] S. Chandrasekhar, *Hydrodynamic and Hydromagnetic Stability*, Oxford University Press, London, 1961.
[5] S. Choi and J. A. Eastman, *Enhancing thermal conductivity of fluids with nanoparticles*, D. A. Siginer and H. P. Wang (Eds.), Development and applications of Non-Newtonian flows", ASME, FED, 231 MD, 66, pp. 99-105, 1995.
[6] M. Corcione, *Rayleigh-Bénard convection heat transfer in nanoparticle suspensions*, Int. J. Heat Fluid Flow, 32, pp. 65-77, 2011.
[7] S. K. Das, N. Putra, P. Thiesen and W. Roetzel, *Temperature dependence of thermal conductivity enhancement for nanofluids*, ASME J. Heat Trans., 125, pp. 567-574, 2003.
[8] J. A. Eastman, S. U. S. Choi, S. Li, W. Yu and L. J. Thompson, *Anomalously increased effective thermal conductivities of ethylene glycol-bases nanofluids containing copper nanoparticles*, Appl. Phys. Lett., 78, pp. 718-720, 2001.
[9] B. Elhajjar, G. Bachir, A. Mojtabi, C. Fakih and M. C. Charrier-Mojtabi, *Modeling of Rayleigh-Bénard natural convection heat transfer in nanofluids*, C. R. Mecanique, 338, pp. 350-354, 2010.
[10] R. L. Hamilton and O. K. Crosser, *Thermal conductivity of heterogeneous two-component systems*, Ind. Eng. Chem. Fund., 1, pp. 187-191, 1962.
[11] R. Y. Jou and S. C. Tzeng, *Numerical research of nature convective heat transfer enhancement filled with nanofluids in rectangular enclosures*, Int. Comm. Heat Mass Trans., 33, pp. 727-736, 2006.
[12] K. Khanafer, K. Vafai and M. Lightstone, *Buoyancy driven heat transfer enhancement in a two-dimensional enclosure utilizing nanofluids*, Int. J. Heat Mass Trans., 46, pp. 3639-3653, 2003.
[13] H. Masuda, A. Ebata, K. Teramae and N. Hishinuma, *Alteration of thermal conductivity and viscosity of liquid by dispersing ultra fine particle*, Netsu Bussei, 7, pp. 227-233, 1993.
[14] M. Nagata, *Bifurcations at the Eckhaus points in two-dimensional Rayleigh-Bénard convection*, Phys. Rev. E, 52, pp. 6141-6145, 1995.
[15] H. M. Park, *Rayleigh-Bénard convection of nanofluids based on the pseudo-single-phase continuum model*, Int. J. Therm. Sci., 90, pp. 267-278, 2015.
[16] P. G. Siddheshwar, C. Kanchana, Y. Kakimoto and A. Nakayama, *Steady finite-amplitude Rayleigh-Bénard convection in nanoliquids using a two-phase model: Theoretical answer to the phenomenon of enhanced heat transfer*, ASME J. Heat Trans., 139, pp. 012402-012411, 2017.
[17] P. G. Siddheshwar, and N. Meenakshi, *Amplitude equation and heat transport for Rayleigh-Bénard convection in Newtonian liquids with nanoparticles*, Int. J. Appl. Comp. Math., 2, pp. 1-22, 2016.
[18] R. K. Tiwari and M. K. Das, *Heat transfer augmentation in a two-sided lid-driven differentially heated square cavity utilizing nanofluids*, Int. J. Heat Mass Trans., 50, pp. 2002-2018, 2007.

P. G. Siddheshwar is a Professor in the Department of Mathematics, Bangalore University, Bengaluru-560056, Karnataka, India. He has more than 100 research papers at his credit on the topic of *linear and non-linear stability of natural convection in Newtonian clear fluids and nanoliquids*.

B. N. Veena is a Junior Research Fellow (JRF) in the Department of Mathematics, Bangalore University, Bengaluru-560056, Karnataka, India. She is in the third year of her Ph. D. program. Her research topic is *Constrained and unconstrained convection of nanoliquid in porous enclosure*.